
A Unified Approach to Obstacle Avoidance and Motion Learning

Anonymous Author(s)

Affiliation

Address

email

Abstract

1 A dynamical system based motion representation for obstacle avoidance and motion
2 learning is proposed. The obstacle avoidance problem can be inverted to
3 enforce that the flow remains enclosed within a given volume. A robot arm can
4 be controlled by using the Γ -field in combination with the converging dynamical
5 system. The closed-form model is extended to time-varying environments, i.e.,
6 moving, expanding and shrinking obstacles. This is applied to an autonomous robot
7 (QOLO) in a dynamic crowd in the center of Lausanne. Using Gaussian Mixture
8 Regression (GMR) motion can be learned by describing them as a combination
9 of local rotations. The motion can be further refined to create a safe invariant set
10 within the obstacles' hull.

1 Introduction

11 Robots navigating in human-inhabited, unstructured environments have to plan or learn the initial
12 path in advance, but they encounter disturbances constantly. In milliseconds a flexible, yet safe
13 control scheme must take the right decisions to avoid collisions.
14

15 Motion learning and collision avoidance is often regarded as two independent problems, i.e., [1]–[3]
16 Recent approaches try to combine these two. Global planning through probabilistic road map (PRM)
17 was extended to dynamic environments through rapid adaptation in [4], but this results in a loss of
18 convergence. Control barrier functions (CBFs) combined with Lyapunov Functions were united
19 through the use of quadratic programming (QP) to create collision-free paths. The QP methods extend
20 the initial controller but are prone to not finding a feasible solution in real-time [5], or introducing a
21 history dependence [6]. A method to modulate initially learned (nonlinear) motion to avoid collisions
22 was introduced in [7], but the approach cannot ensure the absence of local minima in closed-form.

23 We propose a novel approach to unifying learning and obstacle avoidance. On the one hand, the
24 unification allows elevating similarities of the two problems by interpreting both as a modulation
25 of a desired motion towards a goal. On the other hand, the combined approach allows combining
26 learning and avoidance for safe navigation in real-world scenarios while still ensuring convergence
27 constraints.

2 Obstacle Avoidance Formulation

28 Closed-form dynamical systems (DS) have proven suitable for dynamic applications as no re-planning
29 is required. A general dynamical system can be written as a function of the state ξ as:

$$\dot{\xi} = \mathbf{f}(t, \xi) \tag{1}$$

2.1 Obstacle Description

31 Each obstacle has a continuous distance function $\Gamma(\xi) : \mathbb{R}^d \mapsto \mathbb{R}_{\geq 0}$, which allows to distinguish free
32 points ($\Gamma > 1$), boundary points ($\Gamma = 1$), and interior points ($0 < \Gamma < 1$).
33

34 Additionally a reference point ξ_i^r is chosen within its boundaries. This allows to define the reference
 35 direction towards the obstacle as $\mathbf{r}_o(\xi) = (\xi - \xi_i^r) / \|\xi - \xi_i^r\|$.

36 2.2 Obstacle Avoidance through Modulation

37 In [8], real-time obstacle avoidance is obtained by applying a dynamic modulation matrix to a
 38 dynamical system $\mathbf{f}(\xi)$:

$$\dot{\xi} = \mathbf{M}(\xi)\mathbf{f}(\xi) \quad \text{with} \quad \mathbf{f}(\xi) = k(\xi - \xi^a) \quad (2)$$

39 Describing the obstacle avoidance as a modulation of the initial dynamics ensured that attractors are
 40 conserved, i.e. $\mathbf{0} = \mathbf{M}(\xi)\mathbf{0}$. Additionally, no spurious (new) attractors are introduced, as long as the
 41 matrix $\mathbf{M}(\xi)$ has full rank.

42 We will focus on motion with a clearly defined goal (i.e. attractor ξ^a). The scaling parameter k
 43 introduces change with respect to time. It is of unit s^{-1} .

45 2.2.1 Fluid Dynamic Inspired Compression and Stretching

46 The potential (laminar) flow of an incompressible fluid around a cylinder is a known problem
 47 in fluid dynamics with known closed-form description. It will serve as a basis for the obstacle
 48 avoidance algorithm. Similarly to the potential flow, the vector field is scaled in tangent and radial
 49 direction. Hence, the modulation matrix is defined as $\mathbf{M}(\xi) = \mathbf{E}(\xi)\mathbf{D}(\xi)\mathbf{E}(\xi)^{-1}$, a function of the
 50 decomposition matrix $\mathbf{E}(\xi)$ and the diagonal scaling matrix $\mathbf{D}(\xi)$.

51 2.2.2 Modulation through Decoupling of Rotation and Stretching

52 Alternatively, any vector transformation can be interpreted as a rotation with matrix $\mathbf{R}(\xi)$ and a
 53 stretching $h(x)$. This concept has been used in two dimensions for local modulation by [9]:

$$\dot{\xi} = h(\xi)\mathbf{R}(\xi) \mathbf{f}(\xi) \quad (3)$$

54 The rotation can alternatively be applied by using the *orientation-space transform* described in [10]
 55 (instead of the matrix modulation by $\mathbf{R}(\xi)$).

56 2.3 Multiple Obstacles

57 In the presence of multiple obstacles, the velocity is modulated for each obstacle individually. The
 58 final velocity is obtained by taking the weighted mean in direction space in [8]. This has been applied
 59 in Fig. 1.

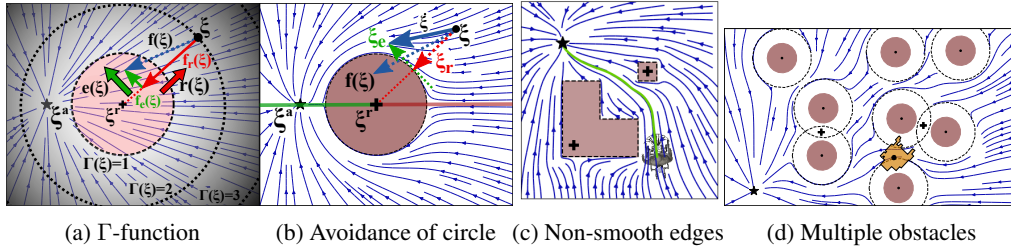


Figure 1: Obstacle avoidance around a single and multiple obstacles.

60 3 Inverted Obstacle Avoidance

61 An autonomous robot might be in a scenario where it has boundaries which cannot be pass. This
 62 might be a wall for a wheeled robot, or it can be safety or joint limits for a robot arm. This is stated as
 63 the constraint of staying within an obstacle, where the boundary of the obstacle represents the limits
 64 of the free space.

65 3.1 Distance Inversion

66 If we use the previously introduced obstacle description to denote enclosing hulls, the interior points
 67 of the classical obstacle become points of free space of the enclosing hull and vice versa. For this
 68 reason, we introduce the inverted distance function Γ^w as:

$$\Gamma^w(\xi) = 1/\Gamma^o = (R(\xi)/\|\xi - \xi^r\|)^{2p} \quad \forall \mathbb{R}^d \setminus \xi^r \quad (4)$$

69 This allows to treat boundaries the previously defined algorithm (but the newly introduced Γ^w). It
 70 follows that convergence is still ensured.

71 3.2 Gaps in the Wall

72 In many practical scenarios a hull entails gaps or holes through which the agent enters or exits the
 73 space (e.g., door in a room). The inverted obstacle avoidance slows the agent down to zero while it
 74 is trying to approach this exit. For this reason, a *guiding reference point* for boundary obstacles is
 75 introduces. It counters this effect and nullifies the avoidance effect close to a gap (see Fig. 2).

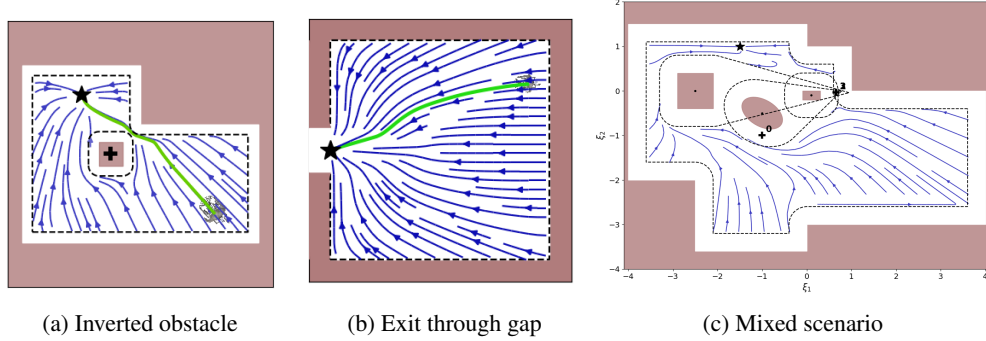


Figure 2: The inverted obstacle description ensures safe navigation within an obstacle (a) and complex environments (c). The introduction of a *guiding reference point* allows exiting through gaps of walls (b).

76 4 Obstacle Avoidance with a Robot Arm

77 The algorithm has so far been described for a point-mass. Extending it to robots which can be
 78 encapsulated in a circular shape is done via a constant margin around all obstacles. The application
 79 to a multiple degree of freedom arm can be done by describing and evaluating it in joint-space.
 80 Alternatively, we introduce a weighted evaluation of the desired dynamics along the links which
 81 ensures a collision-free trajectory towards a desired goal.

82 4.1 Nominal Velocity

83 We assume the successful completion of the task, when the end-effector reaches the attractor, while
 84 avoiding any collisions of the robot arm with the surrounding on the way. The nominal joint velocity
 85 is therefore obtained through inverse-kinematics:

$$\dot{\mathbf{q}}^g = \mathbf{J}^{-1}(\mathbf{q})\dot{\xi}^g \quad (5)$$

86 with Jacobian J , joint state \mathbf{q} and $\dot{\xi}^g = \mathbf{M}(\xi^{ee})\mathbf{f}(\xi^{ee})$ the velocity towards the goal at the end effector
 87 ξ^{ee} .

88 4.2 Danger Field and Weights

89 For the evaluation on the robot arm, the Γ -field is interpreted as a danger-field (similar to [11]).
 90 The danger-field is evaluated at multiple evaluation points along each link, and the corresponding
 91 weight is calculated. The weights are designed to sum up to one in order to balance converging and
 92 avoiding.

93 4.3 Robot Kinematics

94 The velocity of each joint is evaluated starting at the joint closest to the base of the robot and
 95 continuing *joint-by-joint* towards the end-effector. This allows joints higher up the chain to potentially
 96 compensate the avoidance-motion from joints which are lower in the chain (see Fig. 3).

97 5 Dynamic Environment and Application to Crowd

98 In dynamic environments with moving or deforming obstacles, the system is modulated with respect
 99 to a relative velocity:

$$\dot{\xi} = \mathbf{M}(\xi) \left(\mathbf{f}(\xi) - \dot{\xi}^o \right) + \dot{\xi}^o \quad \text{with} \quad \dot{\xi}^o = \dot{\xi}^v + \dot{\xi}^d \quad (6)$$

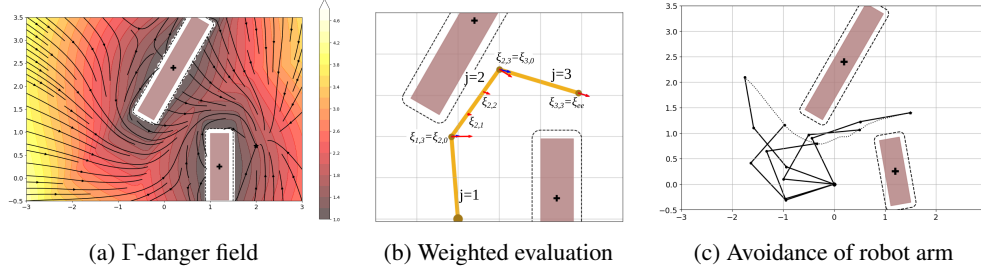


Figure 3: The danger-field (a) is evaluated along the arm of the robot (b). This allows for safe navigation of multiple degree of freedom robot arm in clustered environments (c).

100 The relative velocity consists of the obstacle’s velocity $\dot{\xi}^v$ and deformation $\dot{\xi}^d$. Impenetrability can
 101 be ensured with this approach.

102 5.1 Evaluation in Outdoor Crowds

103 A qualitative proof of concept was performed in an outdoor environment with the QOLO robot
 104 (see [12]) in the center of Lausanne, Switzerland. The location of the experiment is a small market
 105 place with large diversity in both the pedestrian’s velocities and directions of movement. The robot’s
 106 controller is initialized with a linear DS to reach a goal 20 m away from the onset position. Pedestrians
 107 are detected with a camera and LIDAR-based tracker described in [13] (see Fig. 4).

108 We see this as a successful test of the obstacle avoidance algorithm in areal crowd scenario. The robot
 109 managed to pass the crowd without collision during all five trials.¹

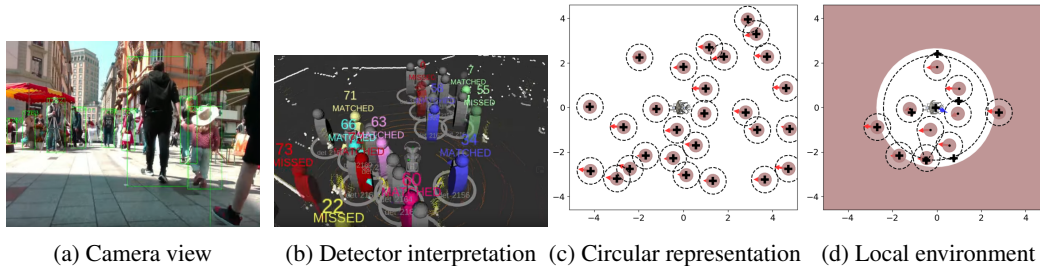


Figure 4: The camera and Lidar (a) are interpreted by the detector to obtain a crowd representation (b). The crowd (c) is then further reduced to a local environment (d) to increase computational speed while ensuring local convergence.

110 6 Extension to Motion Learning

111 The dynamical system frame work has shown to be suitable for motion learning. In combination with
 112 Gaussian Mixture Regression (GMR) complex, yet reactive motion patterns can be learned [2].

113 6.1 Learning the Motion as Local Rotation

114 A motion can be described as a rotation of an initial dynamical system (see Sec. 2). Learning a
 115 regression from recorded data using GMR, the optimal rotation at each position can be predicted.
 116 Using the directional summing described in [10], it can be ensured that the resulting vector field does
 117 not have any spurious attractors.

118 6.2 Learning Boundaries to Create an Invariant Set

119 The Gaussian Mixture Model (which was obtained by the GMR) can be used as the base of a motion
 120 boundary. Ellipses are created with the center aligned with the Gaussians, and the axes lengths are
 121 proportional to the variances of the Gaussians (see Fig. 5). The union of the set of ellipses can be
 122 interpreted as the hull of our learned environment. In combination with the learned motion, this can
 123 now ensure that the motion stays within the invariant set hull. Hence, create a safer and more reactive
 124 model which stays close to the known data.

¹The video can be found under <https://youtu.be/3nbfwcTw8G4>

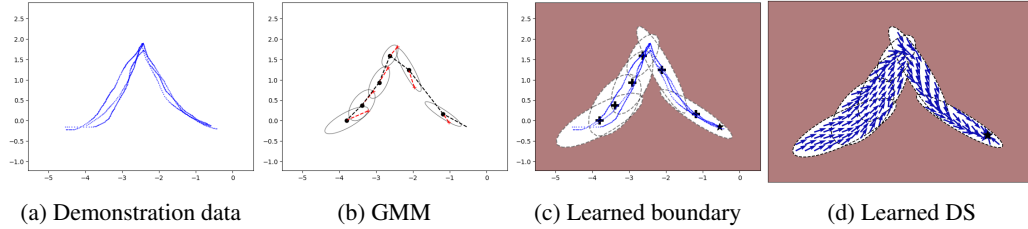


Figure 5: The A-shape of the LASA-dataset (a) is used to obtain corresponding GMM-model (b). This allows the creation of an invariant set (c) to evaluate the dynamics (d).

References

- 125
126 [1] P. Long, W. Liu, and J. Pan, “Deep-learned collision avoidance policy for distributed multiagent naviga-
127 tion,” *IEEE Robotics and Automation Letters*, vol. 2, no. 2, pp. 656–663, 2017.
- 128 [2] S. M. Khansari-Zadeh and A. Billard, “Learning stable nonlinear dynamical systems with gaussian
129 mixture models,” *IEEE Transactions on Robotics*, vol. 27, no. 5, pp. 943–957, 2011.
- 130 [3] K. Neumann and J. J. Steil, “Learning robot motions with stable dynamical systems under diffeomorphic
131 transformations,” *Robotics and Autonomous Systems*, vol. 70, pp. 1–15, 2015.
- 132 [4] J. Vannoy and J. Xiao, “Real-time adaptive motion planning (ramp) of mobile manipulators in dynamic
133 environments with unforeseen changes,” *IEEE Transactions on Robotics*, vol. 24, no. 5, pp. 1199–1212,
134 2008.
- 135 [5] A. D. Ames, J. W. Grizzle, and P. Tabuada, “Control barrier function based quadratic programs with
136 application to adaptive cruise control,” in *53rd IEEE Conference on Decision and Control*, IEEE, 2014,
137 pp. 6271–6278.
- 138 [6] M. F. Reis, A. P. Aguiar, and P. Tabuada, “Control barrier function-based quadratic programs introduce
139 undesirable asymptotically stable equilibria,” *IEEE Control Systems Letters*, vol. 5, no. 2, pp. 731–736,
140 2020.
- 141 [7] S. M. Khansari-Zadeh and A. Billard, “A dynamical system approach to realtime obstacle avoidance,”
142 *Autonomous Robots*, vol. 32, no. 4, pp. 433–454, 2012.
- 143 [8] L. Huber, A. Billard, and J.-J. Slotine, “Avoidance of convex and concave obstacles with convergence
144 ensured through contraction,” *IEEE Robotics and Automation Letters*, vol. 4, no. 2, pp. 1462–1469, 2019.
- 145 [9] K. Kronander, M. Khansari, and A. Billard, “Incremental motion learning with locally modulated
146 dynamical systems,” *Robotics and Autonomous Systems*, vol. 70, pp. 52–62, 2015.
- 147 [10] L. Huber, J.-J. Slotine, and A. Billard, “Avoiding dense and dynamic obstacles in enclosed spaces:
148 Application to moving in a simulated crowd,” *arXiv e-prints*, arXiv–2105, 2021.
- 149 [11] B. Lacevic, P. Rocco, and A. M. Zanchettin, “Safety assessment and control of robotic manipulators
150 using danger field,” *IEEE Transactions on Robotics*, vol. 29, no. 5, pp. 1257–1270, 2013.
- 151 [12] D. F. P. Granados, H. Kadone, and K. Suzuki, “Unpowered lower-body exoskeleton with torso lifting
152 mechanism for supporting sit-to-stand transitions,” in *2018 IEEE/RSJ International Conference on
153 Intelligent Robots and Systems (IROS)*, IEEE, 2018, pp. 2755–2761.
- 154 [13] D. Jia, A. Hermans, and B. Leibe, “Dr-spaam: A spatial-attention and auto-regressive model for person
155 detection in 2d range data,” in *2020 IEEE/RSJ International Conference on Intelligent Robots and
156 Systems (IROS)*, 2020, pp. 10 270–10 277. DOI: 10.1109/IR0S45743.2020.9341689.